

1 **Sexual dimorphism in outcomes of non-muscle invasive bladder cancer: a role of CD163+**
2 **M2 macrophages, B cells and PD-L1 immune checkpoint**

3 Stephen Chenard*^{1,2}, Chelsea Jackson*^{1,3}, Thiago Vidotto⁴, Lina Chen³, Céline Hardy^{1,3}, Tamara
4 Jamaspishvilli^{1,3}, David Berman^{1,2,3}, D. Robert Siemens^{1,2,5}, Madhuri Koti^{1, 2, 5**}

5
6 **Affiliations**

7 ¹Queen's Cancer Research Institute, Kingston, ON, Canada; ²Department of Biomedical and
8 Molecular Sciences, Queen's University, Kingston, ON, Canada; ³Department of Pathology and
9 Molecular Medicine, Queen's University, Kingston, ON, Canada; ⁴Department of Pathology,
10 Johns Hopkins School of Medicine, USA; ⁵Department of Urology, Queen's University, Kingston,
11 ON, Canada

12
13 **Equal contribution*

14
15 ****Address for correspondence**

16 Madhuri Koti, DVM, MVSc, PhD

17 Assistant Professor

18 Department of Biomedical and Molecular Sciences and Obstetrics and Gynecology

19 Queen's Cancer Research Institute

20 Queen's University, Kingston, Ontario K7L3N6

21 Canada

22 e-mail: kotim@queensu.ca

23

24 **Abstract**

25 Non-muscle invasive bladder cancer (NMIBC) is significantly more common in men than women.
26 However, female patients with NMIBC often present with more aggressive disease and do not
27 respond as well to immunotherapy treatments. We hypothesized that sexual dimorphism in the
28 tumor immune microenvironment (TIME) may contribute to the inferior clinical outcomes
29 observed in female patients. To test this hypothesis, we interrogated the expression patterns of
30 genes associated with specific immune cell types and immune regulatory pathways using tumor
31 whole transcriptome profiles from male (n=357) and female (n=103) patients with NMIBC. High-
32 grade tumors from female patients exhibited significantly increased expression of *CD40*, *CTLA4*,
33 *PDCD1*, *LAG3* and *ICOS* immune checkpoint genes. Based on the significant differences in
34 expression profiles of these genes and the cell types that most commonly express these in the
35 TIME, we evaluated the density and spatial distribution of CD8+Ki67+ (activated cytotoxic T
36 cells), FoxP3+ (regulatory T cells), CD103+ (tissue resident T cells), CD163+ (M2-like tumor
37 associated macrophages), CD79a+ (B cells), PD-L1+ (Programmed-Death Ligand-1) and PD-1+
38 cells using multiplexed immunofluorescence in an independent cohort of 332 patient tumors on a
39 tissue microarray (n=259 males and n=73 females). Tumors from female patients showed
40 significantly higher infiltration of CD163+ macrophages and PD-L1+ cells compared to tumors
41 from male patients. Notably, increased infiltration of CD163+ macrophages and CD79a+ B cells
42 independently associated with decreased recurrence free survival. Not only do these results have
43 the potential to inform the rational utilization of immunomodulatory therapies based on the TIME
44 of both male and female patients with NMIBC, these novel findings highlight the necessity of
45 considering sexual dimorphism in the design of future immunotherapy trials.

46

47 **Introduction**

48 In 2018, bladder cancer was the 10th most common cancer worldwide, with an estimated
49 549,000 newly diagnosed cases and approximately 200,000 deaths caused by the disease [1]. Over
50 90% of bladder tumors arise from the urothelial cells that line the bladder. Localized urothelial
51 carcinoma of the bladder (UCB) can be broadly categorized based on the depth of tumor invasion;
52 approximately 75% of incident cases present as non-muscle-invasive bladder cancer (NMIBC),
53 while the rest are classified as muscle-invasive disease [2].

54 The gold-standard first-line treatment for NMIBC is transurethral resection of bladder
55 tumor (TURBT) surgery. Following surgical resection, patients diagnosed with high-risk features
56 (such as high stage, grade, or tumor multifocality) [3] are best treated with intravesical Bacillus
57 Calmette-Guérin (BCG) immunotherapy. BCG is a live-attenuated form of *Mycobacterium bovis*
58 (*M. bovis*) and is commonly used as a vaccine for the prevention of tuberculosis. While NMIBC
59 is four times more common in men, women suffer earlier recurrences following treatment with
60 BCG immunotherapy and experience shorter progression-free survival (PFS) when compared to
61 their male counterparts [4–6]. Clearly, patient sex (biological differences) and gender
62 (social/behavioral differences) are associated with the incidence and clinical outcomes of NMIBC;
63 however, these factors are understudied in biomarker and treatment design [7].

64 The pre-treatment tumor immune microenvironment (TIME) is a critical determinant of
65 response to immunomodulation in several cancer types [8], and potentially plays a similar role in
66 determining the response of bladder cancer patients to treatment with BCG immunotherapy [9,10].
67 The evolution of variable TIME states across the spectrum of non-inflamed (low/no immune
68 infiltration) to inflamed (high immune cell infiltration) tumors depends on host and/or cancer cell
69 intrinsic factors that influence the recruitment and functional states of immune cells [11]. Aligning

70 with this concept and in the context of contemporary immunomodulatory agents including the PD-
71 1/PD-L1 targeting immune checkpoint blockade therapy, patient biological sex has recently
72 emerged as an important factor in response to treatment [12–14]. Under normal physiological
73 conditions, macrophages are the most abundant resident innate immune cells within the bladder
74 mucosa. Pre-clinical studies in murine models have shown that females exhibit higher magnitude
75 of immune responses to urinary pathogens than males [15]. Advancing age, microbial challenges,
76 host genetics and post-menopausal hormonal changes also contribute to increased recruitment of
77 adaptive immune cell populations, within the bladders of females. Despite mounting evidence of
78 the importance of these cell types in response to immunomodulatory therapy in several other
79 cancers, their sex-specific roles and functional states within the NMIBC TIME have yet to be fully
80 elucidated.

81 We hypothesized that sexual dimorphism in clinical outcomes of NMIBC are driven by
82 differences in the TIME. To test this hypothesis, we evaluated the association between patient sex
83 and available clinical outcomes in two independent cohorts of NMIBC; UROMOL (publicly
84 available dataset of tumors from 460 patients) [16] and Kingston Health Sciences Center (KHSC;
85 332 patients). We then evaluated the tumor transcriptome profiles of the UROMOL cohort to
86 determine sex associated differences in immune regulatory genes. Guided by the findings from
87 immune regulatory gene expression patterns, we further investigated the density and spatial
88 distribution of selected immune cell populations and immune checkpoint proteins in tumors from
89 male and female patients in the KHSC cohort. Findings from our study provide the first evidence
90 for sex associated differences in the TIME of NMIBC.

91

92 **Results**

93 *Female patients with high grade NMIBC tumors exhibit shorter progression free survival*

94 We evaluated the association between patient sex and available clinical outcomes in two
95 independent cohorts of NMIBC; UROMOL (460 patients) [16] and KHSC (332 patients). Clinical
96 features of the KHSC cohort are presented in **Table S1**, whereas those for the UROMOL cohort
97 were previously reported [16]. In the KHSC cohort, 22% of the patients were female, 60% of the
98 entire cohort had high-grade disease (Supplementary **Table S2**) at original presentation and the
99 majority (88%) did not have evidence of BCG immunotherapy prior to collection of their
100 specimens (BCG naïve). Approximately 38% of patients received one or more doses of BCG
101 (**Table S1**). Clinical care of all patients was coordinated at a single treatment clinic and decisions
102 regarding adjuvant therapies were based on AUA risk score. The UROMOL cohort had a similar
103 proportion of female patients (22%). The proportions of patients who underwent BCG
104 immunotherapy was 19% and 54% in the UROMOL and KHSC cohorts, respectively. In alignment
105 with previous reports on sex associated differential outcomes, female patients with high-grade
106 NMIBC had a shorter PFS compared to males in both the cohorts (**Figure 1A and 1B**).

107

108 *High grade tumors from female patients with NMIBC exhibit increased expression of immune* 109 *regulatory genes*

110 Using whole transcriptome profiles of tumors in the UROMOL cohort (n= 103 female and
111 357 male), a targeted analysis was performed to determine grade- and sex-associated differential
112 expression patterns of genes identifying immune cell phenotypes (specifically macrophages, T
113 cells, and B cells), their functional states, and immune-regulatory functions [17]. Significantly

114 higher expression of the immune checkpoint genes *CTLA4*, *PDCDI*, *LAG3* and *ICOS*, were
115 observed in high-grade tumors from females compared to those from males and compared to low-
116 grade tumors from both sexes (**Figure 1C**). Importantly, transcript levels of B cell recruiting
117 chemokine, *CXC ligand 13 (CXCL13)* and B cell surface-associated molecule, *CD40* were
118 significantly increased in high-grade tumors from female patients (**Figure 1C**).

119

120 ***Tumors from female patients with NMIBC have increased CD163+ M2-like macrophages,***
121 ***CD79a+ B cells and higher PD-L1 immune checkpoint protein expression***

122 Based on the differences in immunoregulatory gene expression profiles investigated in the
123 UROMOL cohort, we next evaluated sex-associated differences in the density and localization of
124 a subset of immune cells that are known to express the relevant phenotypic markers and immune
125 checkpoint proteins, and have the potential to secrete the cytokine CXCL13. As such, we
126 investigated the epithelial and stromal density profiles of T helper (CD3+CD8-), T cytotoxic
127 (CD8+Ki67-, activated CD8+Ki67+), T regulatory (CD3+CD8- FOXP3+), tissue resident T
128 (CD103+), B-cells (CD79a), M2-like tumor associated macrophages (TAMs, CD163+) and
129 immune checkpoint proteins (PD-L1 and PD-1) in tumors from the KHSC cohort.

130 Interestingly, among all the immune cell phenotypes, only CD163+ M2-like TAMs
131 demonstrated statistically significant differences in the density and localization between both low
132 grade and high-grade tumors from male and female patients. A significantly higher infiltration of
133 CD163+ TAMs was seen in the epithelial compartment of low-grade tumors (p=0.012) and in both
134 epithelial and stromal compartments of high-grade tumors (p= 0.001, p<0.001, respectively) from
135 female patients compared to those from male patients (**Figure 1D**). Density of CD79a+ B cells

136 was not significantly different between sexes; however, CD79a+ B cell infiltration was higher in
137 the epithelial and stromal compartments ($p < 0.001$) of high-grade tumors compared to low-grade
138 tumors from both sexes (**Figure 1E**). Importantly, tumors from female patients exhibiting
139 recurrence within one year showed significantly higher density of CD163+ TAMs compared to
140 those from males (**Figure 1F**). With respect to CD79a+ B cells, a trend towards higher infiltration
141 was observed in tumors from female patients who recurred within 1 year of BCG treatment (**Figure**
142 **1F**). Spearman correlation analysis showed a moderate positive correlation ($r = 0.63$) between
143 stromal CD79a+ B cells and CD163+ TAMs (**Figure 1G**).

144 PD-L1 protein expression was significantly higher in both the epithelial and stromal
145 compartments of high-grade tumors compared to low-grade tumors (**Figure 1H**; $p < 0.001$).
146 However, apparent sex-associated differences in PD-L1 protein expression (especially in the
147 epithelial compartment) were likely not statistically significant due to the wide variability in the
148 proportion of PD-L1+ cells.

149 A subset analysis of cases was performed on patients that had no evidence of previous
150 intravesical BCG immunotherapy (BCG naïve) by excluding from the entire cohort those patients
151 that had documented BCG prior to specimen collection or where that data could not be definitely
152 determined. Trends in infiltration profiles of CD163 and CD79a between grades and between sexes
153 were consistent with those seen in the whole cohort (**Supplementary Figures 2A-C**) although in
154 this analysis expression of PD-L1 protein in the epithelial compartment of low-grade tumors from
155 females was significantly higher compared to males ($p = 0.04$).

156

157 *T helper and regulatory cells exhibit significant sex differences in density and spatial*
158 *distribution within the NMIBC TIME*

159 While we observed no sex-associated differences in the density and spatial organization of
160 CD8+ cytotoxic T cells, CD3+CD8- T helper cells and CD3+CD8-FoxP3+ T regulatory cells were
161 significantly higher in low-grade tumors from female patients compared to those from males
162 (Supplementary Fig. 3A and B). Such differences were not observed in high-grade tumors.

163

164 **Increased density of CD163+ M2-like macrophages and CD79a+ B cells associates with early**
165 **recurrence in NMIBC**

166 Kaplan-Meier analysis for all patients with high-grade NMIBC (n=170) in the KHSC cohort
167 showed that, irrespective of their localization in the stroma or epithelium, higher density
168 (Supplementary **Table S2**) of CD163+ M2-like TAMs (**Figure 2A**) and CD79a+ B cells (**Figures**
169 **2B**) independently associated with shorter recurrence free survival (RFS). This association was
170 observed in both male and female patients supporting the notion that rather than being a sexually
171 dimorphic epiphenomenon, these cells may play a functional role in tumor recurrence (**Figures**
172 **2C and 2D**). Notably, these differences in RFS remained consistent using similar thresholds for
173 both CD79a+ and CD163+ cells, in all patients with high-grade tumors (**Supplementary Figures**
174 **4a, 4b, 5a and 5b**).

175

176

177

178 **Discussion**

179 In the current study, we report the first demonstration of sexual dimorphism in the TIME
180 of NMIBC. In concordance with previous reports [4–6], we found that female patients with high-
181 grade NMIBC suffer from shorter progression free survival as compared to their male counterparts.
182 Analysis of a panel of immune regulatory genes (both stimulatory and inhibitory) in tumors from
183 the UROMOL cohort demonstrated increased expression of immune checkpoint genes, and those
184 associated with B cell recruitment and function in high-grade tumors from females compared to
185 those from males. These alterations are indicative of an exhausted immune landscape following
186 an increased activation within the NMIBC TIME. Given the dynamic nature of immune checkpoint
187 gene expression, variability in checkpoint co-expression, and an expected lack of direct correlation
188 with protein level expression, we investigated the profiles of cell types known to express these
189 molecules following activation or exhaustion.

190 Our finding of higher infiltration of CD163+ M2-like suppressive TAMs in tumors from
191 female patients may partially explain the overall poor clinical outcomes experienced by female
192 patients following BCG immunotherapy. A significantly increased density of M2-like TAMs in
193 tumors from female patients may be driven by differences dictated by sexual dimorphism in overall
194 bladder mucosal immune physiology [15]. Indeed, higher infiltration of tumors by CD163+ M2-
195 like TAMs has been previously reported to be associated with poor clinical outcomes in NMIBC
196 [18]. It is also known that bladder cancer cells induce the polarization of tissue-resident and
197 reactive macrophages [19], potentially influencing tumor progression and treatment response [20].
198 Our novel findings of the higher density of B cells in tumors from female patients are reflective of
199 the established physiological links between M2-like TAMs and B cells [21]; co-stimulation of M2-
200 like macrophages with bacterial lipopolysaccharide and IL-10 induces production of CXCL13, a

201 chemokine critical for B cell recruitment [22,23]. Given the increased incidence of urinary tract
202 infections in women – and the cancer cell-induced polarization of TAMs towards an M2-like
203 phenotype [19] – it is plausible that increased engagement of M2-like TAMs by urinary pathogens
204 leads to increased CXCL13 secretion and B cell recruitment in tumors of female NMIBC patients.
205 Eventually, these recruited cells acquire a dysfunctional or exhausted phenotype, persisting in an
206 immunological stalemate within the NMIBC TIME. This observation is further strengthened by
207 our *in silico* transcriptomic analysis showing increased expression of *CXCL13*, however, further
208 mechanistic evidence is warranted. Similarly, it is also known that IL-10 secreted by B regulatory
209 cells inhibits macrophage activation and polarizes them towards an M2-like phenotype [24].
210 Indeed, under normal physiological conditions, females exhibit higher proportions of B cells and
211 increased responsiveness to BCG vaccination [25,26]. However, given the older age of patients
212 with NMIBC, it is possible that a reduced naïve B cell pool in the periphery [27] compromises the
213 desired responses in the NMIBC scenario following local BCG administration in contrast to
214 responses associated with infant vaccination. We acknowledge that the static TIME states
215 evaluated in this study, however, do not provide definitive evidence supporting these temporal
216 phenomena and warrant further investigation.

217 Another novel finding from our study is the inverse association of B cells and CD163+
218 M2-like TAMs with recurrence free survival in BCG naïve patients. This finding has significant
219 implications in advancing the current state of knowledge on the antigen presenting function of
220 these cells following encounter with BCG bacteria upon their intra-vesical administration. For
221 example, it is known that M2-like macrophages exhibit tolerance and are unable to secrete
222 CXCL10 [28], which limits their ability to recruit immune cells to the TIME. However, BCG
223 treatment has been shown to re-program M2 macrophages [29] that may lead to some degree of

224 the observed anti-tumor responses. B cells have been shown to be indicators of good prognosis in
225 certain cancers [30,31]. However, their anti-tumor roles likely depend either on their antibody
226 producing or antigen presentation function, neither of which are well understood in NMIBC. The
227 negative prognostic association of B cells, as observed in this study, indicates their potentially
228 exhausted or regulatory phenotype. A comprehensive analysis of their functional states is needed
229 to define their tumor killing or promoting roles.

230 Another important finding from this study is the sex-associated difference in PD-L1 protein
231 expression. PD-L1 is known to be expressed on a wide variety of immune cells and cancer cells
232 and is partially regulated by estrogen and X-linked microRNAs [32,33]. Indeed, pre-treatment PD-
233 L1 expression was recently shown to be predictive of response to BCG [34]. The current finding
234 suggesting overall higher PD-L1 expression in tumors from females may inform more precise use
235 of combination therapies targeting this immune checkpoint in female patients despite the
236 challenges due to the dynamic nature of its expression.

237 The current findings should inform immunotherapy trials that are adequately powered to
238 evaluate responses in female patients with NMIBC. Increased abundance of CD163+ M2-like
239 macrophages may also explain the compounding effects of these suppressive factors that impart
240 an aggressive behavior leading to poor clinical outcomes experienced by female patients relative
241 to males. Several trials targeting CD40 or CSF1R (M2 TAM targeting) in combination with PD-
242 L1 immune checkpoint blockade are underway in a variety of cancers [35], outcomes of which
243 might inform their potential use in NMIBC.

244 Our study is not without limitations. PD-L1 immune checkpoint is expressed on a wide
245 variety of cells including cancer and immune cells in the TIME. Future studies evaluating the co-

246 localization of immune checkpoint should derive definitive information on cell types expressing
247 this immune checkpoint. Furthermore, a more comprehensive evaluation of the functional states
248 of immune cells and immunogenomic correlates driving their recruitment via cell intrinsic
249 interferon activation, is needed to guide more precise therapeutic targeting. Nevertheless, findings
250 from this study have significant implications in ongoing immune checkpoint blockade trials where
251 sex-associated pre-treatment tumor immune landscape could inform their precise use in drug
252 sequencing.

253

254 **Methods**

255 *Patient Cohorts and Clinical Data*

256 This study was approved by the Ethics Review Board at Queen's University. A cohort of 509
257 NMIBC archival transurethral bladder tumors (TURBTs) from 332 patients between 2008-2016
258 was collected from Kingston Health Sciences Center (KHSC). Stage Ta and T1 tumors were
259 included following pathological review (DMB and LC), using the WHO 2016 grading system [36].
260 Clinical details of the UROMOL cohort were previously reported by Hedegaard et al. 2016 [16].
261 Six tissue microarrays (TMA) were constructed with duplicate 1.0 mm cores. Recurrence was
262 defined as time from each patient's earliest TURBT resection to next malignant diagnosis.
263 Operative notes were reviewed to exclude re-resections as recurrences.

264 *Multiplex Immunofluorescence Staining for Immune Markers*

265 TMAs were stained with three panels of primary-conjugated fluorescent antibodies. The first panel
266 contained antibodies against CD3+, CD8+, Ki67+, and FoxP3+ cells. The second panel contained

267 antibodies against PD-1+, PD-L1+, and CK5+ cells. The third panel contained antibodies against
268 CD163+, CD79a+, CD103+, and GATA3+ cells. Expression for the following cell types and
269 immune checkpoints were evaluated in the epithelial and stromal compartments: T-cells
270 (CD3+CD8+Ki67, CD3+CD8+Ki67+, CD3+CD8-FOXP3-, CD3+CD8-FOXP3+), immune
271 checkpoint (PD-1+, PDL1+, CK5+PDL1+), B-cells (CD79a+), M2-like TAMs (CD163+), and
272 tissue-resident T cells (CD103+). The presence of these immune markers was evaluated for each
273 core by automated multiplex immunofluorescent staining at the Molecular and Cellular
274 Immunology Core (MCIC) facility, BC Cancer Agency. All antibodies were provided by Biocare
275 Medical (Pacheco, CA, USA) and distributed by Inter Medico (Markham, ON, CAN).

276 *Automated Scoring of Multiplex Immunofluorescence Staining for Immune Markers*

277 The stained TMA sections were scanned using the Vectra multispectral imaging system. Tissue
278 segmentation into stromal and epithelial compartments was performed using PerkinElmer's
279 InForm software. Ten randomly selected cores were utilized to train three independent algorithms
280 in PerkinElmer's InForm software package. The InForm software identified positive pixels for all
281 of the selected immune markers using each of the three independent algorithms. The average of
282 the three independent algorithms was taken for all three sets of immune markers in each core.
283 Cores that were missing $\geq 75\%$ of the tissue were excluded from further analyses.

284 *Manual Validation of Automated Scoring of Multiplex Immunofluorescence Staining*

285 Standard deviation between the three algorithms was calculated for each of the immune markers
286 within both the epithelial and stromal compartments. Outliers were identified and cross-referenced
287 with the composite image of the corresponding TMA core to verify the discrepancy before
288 excluding the outlying data points from further analysis. Any quantifications that included

289 misidentification of histological artifacts as immune cells by any of the three algorithms were also
290 excluded from analysis. Algorithms that consistently over-called or under-called the immune
291 marker quantification were excluded from analysis. Further visual validation of the automated
292 scoring was performed for randomly selected TMA cores.

293 *RNAseq Gene Expression Analysis*

294 Raw RNAseq data from 460 NMIBC samples [16], were downloaded
295 (<https://www.ebi.ac.uk/ega/studies/EGAS00001001236>), and VST normalized data were obtained
296 by employing the vst function on DESeq2 in R v4.0.1. Further, we compiled a list comprising
297 immune-cell markers and regulatory genes based on our previous report [17]. We then compared
298 the expression of these VST-normalized genes between four groups of patients: high-grade
299 females, low-grade females, high-grade males, and low-grade males. The Kruskal-Wallis test was
300 employed to determine significant differences between the two four groups.

301 *Statistical Analysis*

302 Analyses were conducted using R version 3.5.3. Kaplan-Meier curves were plotted using log-rank
303 statistics with survival and survminer packages. Follow-up time for Kaplan-Meier curves ended
304 when 10% of patients remained in each group [37]. Log-rank statistics were used to optimize
305 thresholds for ideal number of CD163+ M2-like TAMs/CD79a+ B cells associated with shorter
306 recurrence-free survival, using the maxstat package in R. Optimal thresholds are summarized in
307 **Supplemental Table S3.**

308

309 **Conflicts of Interest**

310 The authors declare no conflicts of interest.

311 **Acknowledgements**

312 This work is supported by the Early Researcher Award; Ontario Ministry of Research Innovation
313 and Science and the Mary and Mihran Basmajian award for Excellence in Health Research, ,
314 Queen's University to MK and SEAMO Innovation award to DRS and MK.

315

316 **Figure legends**

317 **Figure 1. Patients with NMIBC exhibit sexual dimorphism in progression free survival and**
318 **tumor immune microenvironment.**

319 (A-B) Kaplan Meier survival curves showing female patients with high-grade NMIBC experienced
320 significantly ($P < 0.001$) shorter PFS than their male counterparts and patients with low-grade
321 tumors, in both the UROMOL (A) and KHSC (B) cohorts. Kaplan-Meier survival analyses was
322 performed using log-rank statistics with survival and survminer packages.

323 (C) High-grade tumors from female patients in the UROMOL cohort exhibit significantly
324 increased expression of immunoregulatory genes, *CXCL13*, *PDCD1*, *CD40*, *CTLA4*, and *ICOS*.
325 VST-normalized genes between four cohorts: high-grade cancer in females (HG_F), low-grade
326 cancer in females (LG_F), high-grade cancer in males (HG_M), and low-grade cancer in males
327 (LG_M) are shown. The Kruskal-Wallis test was employed to determine statistically significant
328 differences.

329 (D-E) Violin plots of mean cell counts for CD163+, CD79a+ cell and PD-L1+ cell populations
330 respectively, in the epithelial (left) and stromal (right) compartments of tumors from the KHSC
331 cohort. Plots stratified by low-grade and high-grade samples for males (blue) versus females
332 (pink). Significant differences signified by asterisks between grades (with bracket) and between

333 sexes (no bracket) as determined by Mann-Whitney-U test. ***p-value < 0.001, **p-value < 0.01,
334 *p-value < 0.05.

335 (F) In a subset of patients from the KHSC cohort that recurred in <1 year, female patients had
336 significantly higher density of CD163+ cells in the stroma and epithelium, while there were no
337 significant sex-associated differences in CD79a+ cells. *p-value < 0.05.

338 (G) Spearman correlation plot for CD163+, CD79a+ and PD-L1+ populations in the epithelial
339 (Epi) and stromal (Str) compartments of tumors from the KHSC cohort. Dark blue indicates a
340 positive correlation coefficient (>1), dark red indicates a negative correlation coefficient (<1).

341 (H) Violin plots of mean cell counts for PD-L1+ cell populations in the epithelial (left) and stromal
342 (right) compartments of tumors from the KHSC cohort. Plots stratified by low-grade and high-
343 grade samples for males (blue) versus females (pink). Differences between grades in each
344 compartment as determined by Mann-Whitney-U test ***p-value < 0.001.

345

346 **Figure 2. Recurrence free survival (RFS) in high-grade non-muscle invasive bladder cancer**
347 **is associated with patient sex and tumor immune microenvironment.**

348 (A) Kaplan Meier survival curves for RFS of patients with high-grade NMIBC (n=193) based on
349 log-rank optimized thresholds for density of CD163+ cells in tumor epithelial (left; P<0.001) and
350 stromal (right; P<0.001) compartments. Of this entire cohort, 74% had evidence of adequate BCG
351 therapy after specimen collection (TURBT).

352 (B) Kaplan Meier survival curves showing RFS of high-grade patients based on log-rank optimized
353 thresholds for epithelial (left; P<0.01) and stromal (right; P<0.0001) CD79a+ cells.

354 (C) Kaplan Meier survival curves showing RFS of high-grade patients based on log-rank optimized
355 thresholds for stromal (left; $P < 0.01$) and epithelial (right; $P = 0.014$) CD163+ cells stratified by sex.
356 High vs low stromal CD163+ cells defined as > 64 or < 64 cells, respectively. High versus low
357 epithelial CD163+ cells defined as > 12 or < 12 cells, respectively.

358 (D) Kaplan Meier survival curves showing RFS of high-grade patients based on log-rank
359 optimized thresholds for stromal (left; $P < 0.001$) and epithelial (right; $P = 0.028$) CD79a+ cells
360 stratified by sex. High versus low stromal CD79a+ cells defined as > 35 or < 35 cells, respectively.
361 High vs low epithelial CD79a+ cells defined as > 3 or < 3 cells, respectively.

362

363 **Supplementary Figures**

364 **Supplementary Figure 1. Multiplex immunofluorescence staining and automated tissue**
365 **segmentation of representative tumor core.** A composite view of a representative tumor core,
366 highlighting antibody panels distinguishing CD3+CD8+Ki67+/- and CD3+CD8-FoxP3- cells (A);
367 CD79a+ B, CD103+ T resident and CD163+ M2-like TAMs (B); PD-1+, PD-L1+ and CK5+ cells
368 (C). PerkinElmer's Inform software based automated segmentation of tumor core into epithelial
369 (red) and stromal (green) compartments prior to automated scoring of positively stained cells (D).

370 **Supplementary Figure 2. Profiles of CD163, CD79a and PD-L1 in tumors from BCG naïve**
371 **patients**

372 Violin plots of mean cell counts for CD163+ (A), CD79a+ (B) and PD-L1+ cell (C) populations
373 respectively, in the epithelial (left) and stromal (right) compartments of tumors from the KHSC
374 cohort with no evidence of BCG immunotherapy prior to collection of their specimens (BCG

375 naïve). Asterisks indicate level of significance as determined by Mann-Whitney-U statistics: ***p-
376 value < 0.001 **p-value < 0.01 *p-value < 0.05.

377 **Supplementary Figure 3. Profiles of T helper (3A) and T regulatory (3B) cells in tumors from**
378 **BCG naïve patients and overall cohort**

379 Violin plots of mean cell counts for CD3+CD8- T helper (A) and CD3+CD8-FoxP3+ T regulatory
380 cells (B) in BCG naïve and overall cohort. Plots stratified by low-grade and high-grade samples
381 for males (blue) versus females (pink). Asterisks indicate level of significance as determined by
382 Mann-Whitney-U statistics: ***p-value < 0.001 **p-value < 0.01 *p-value < 0.05.

383 **Supplementary Figure 4. CD79a+ B cell density is associated with recurrence free survival**
384 **in patients with high-grade NMIBC and no prior history of BCG before specimen collection**
385 **(BCG naïve).**

386 (a) Recurrence-free survival of a subset of patients with high-grade disease and no previous BCG
387 therapy prior to specimen collection (n=170). Within this cohort 74% had evidence of adequate
388 BCG therapy after specimen collection (TURBT). Based on log-rank optimized cut-offs for
389 stromal (left; p<0.001) and epithelial (right; p<0.056) CD79a+ cells stratified by males (blue)
390 versus females (pink).

391 (b) Recurrence-free survival based on log-rank optimized cut-offs for stromal (left) and epithelial
392 (right) CD79a+ cells stratified by high CD79a+ cells versus low CD79a+ cells. High versus low
393 stromal CD79a+ cells defined as > 35 or < 35 cells, respectively. High vs low epithelial CD79a+
394 cells defined as > 3 or < 3 cells, respectively. Associated p-values for the epithelial and stromal
395 compartments is <0.01 and <0.0001, respectively.

396 **Supplementary Figure 4. Higher CD163+ cell infiltration is associated with shorter**
397 **recurrence free survival in BCG-naïve patients with high-grade NMIBC.**

398 (a) Recurrence-free survival of high-grade, BCG naïve patients (n=170) based on log-rank
399 optimized cut-offs for stromal (left; P=0.017) and epithelial (right; 0.057) CD163+ cells stratified
400 by males (blue) versus females (pink).

401 (b) Recurrence-free survival based on log-rank optimized cut-offs for stromal (left) and epithelial
402 (right) CD163+ cells stratified by high CD163+ cells versus low CD163+ cells. High versus low
403 stromal CD163+ cells defined as > 64 or < 64 cells, respectively. High vs low epithelial CD163+
404 cells defined as > 12 or < 12 cells, respectively. Associated p-values for the epithelial (right) and
405 stromal (left) compartments are both p<0.01.

406

407 **Supplementary Tables**

408 **S1. Clinical characteristics of patients in the KHSC cohort (n=332).**

409 **S2. Sample characteristics (grade, stage and sex) for overall KHSC cohort (n = 509)**

410 **S3. Optimized log-rank thresholds for recurrence-free survival for individual immune**
411 **markers**

412

413

414

415 **References**

- 416 [1] Bray F, Ferlay J, Soerjomataram I, Siegel RL, Torre LA, Jemal A. Global cancer statistics
417 2018: GLOBOCAN estimates of incidence and mortality worldwide for 36 cancers in 185
418 countries. *CA Cancer J Clin* 2018;68:394–424. <https://doi.org/10.3322/caac.21492>.
- 419 [2] Woldu SL, Bagrodia A, Lotan Y. Guideline of guidelines: non-muscle-invasive bladder
420 cancer. *BJU Int* 2017;119:371–80. <https://doi.org/10.1111/bju.13760>.
- 421 [3] Sylvester RJ, van der Meijden APM, Oosterlinck W, Witjes JA, Bouffouix C, Denis L, et
422 al. Predicting recurrence and progression in individual patients with stage Ta T1 bladder
423 cancer using EORTC risk tables: a combined analysis of 2596 patients from seven
424 EORTC trials. *Eur Urol* 2006;49:466–7. <https://doi.org/10.1016/j.eururo.2005.12.031>.
- 425 [4] Uhlig A, Strauss A, Seif Amir Hosseini A, Lotz J, Trojan L, Schmid M, et al. Gender-
426 specific Differences in Recurrence of Non-muscle-invasive Bladder Cancer: A
427 Systematic Review and Meta-analysis. *Eur Urol Focus* 2018;4:924–36.
428 <https://doi.org/10.1016/j.euf.2017.08.007>.
- 429 [5] Marks P, Soave A, Shariat SF, Fajkovic H, Fisch M, Rink M. Female with bladder cancer:
430 what and why is there a difference? *Transl Androl Urol* 2016;5:668–82.
431 <https://doi.org/10.21037/tau.2016.03.22>.
- 432 [6] Kluth LA, Fajkovic H, Xylinas E, Crivelli JJ, Passoni N, Rouprêt M, et al. Female gender
433 is associated with higher risk of disease recurrence in patients with primary T1 high-grade
434 urothelial carcinoma of the bladder. *World J Urol* 2013;31:1029–36.
435 <https://doi.org/10.1007/s00345-012-0996-9>.

- 436 [7] Saginala K, Barsouk A, Aluru JS, Rawla P, Padala SA, Barsouk A. Epidemiology of
437 Bladder Cancer. *Med Sci (Basel, Switzerland)* 2020;8.
438 <https://doi.org/10.3390/medsci8010015>.
- 439 [8] Binnewies M, Roberts EW, Kersten K, Chan V, Fearon DF, Merad M, et al.
440 Understanding the tumor immune microenvironment (TIME) for effective therapy. *Nat*
441 *Med* 2018;24:541–50. <https://doi.org/10.1038/s41591-018-0014-x>.
- 442 [9] Annels NE, Simpson GR, Pandha H. Modifying the Non-muscle Invasive Bladder Cancer
443 Immune Microenvironment for Optimal Therapeutic Response. *Front Oncol* 2020;10:175.
444 <https://doi.org/10.3389/fonc.2020.00175>.
- 445 [10] Roumigué M, Compérat E, Chaltiel L, Nouhaud FX, Verhoest G, Masson-Lecomte A, et
446 al. PD-L1 expression and pattern of immune cells in pre-treatment specimens are
447 associated with disease-free survival for HR-NMIBC undergoing BCG treatment. *World J*
448 *Urol* 2020. <https://doi.org/10.1007/s00345-020-03329-2>.
- 449 [11] Giraldo NA, Sanchez-Salas R, Peske JD, Vano Y, Becht E, Petitprez F, et al. The clinical
450 role of the TME in solid cancer. *Br J Cancer* 2019;120:45–53.
451 <https://doi.org/10.1038/s41416-018-0327-z>.
- 452 [12] Conforti F, Pala L, Bagnardi V, Pas T De, Martinetti M, Viale G, et al. Articles Cancer
453 immunotherapy efficacy and patients' sex : a systematic review and meta-analysis
454 2018;4:1–10. [https://doi.org/10.1016/S1470-2045\(18\)30261-4](https://doi.org/10.1016/S1470-2045(18)30261-4).
- 455 [13] Wang C, Qiao W, Jiang Y, Zhu M, Shao J, Ren P, et al. Effect of sex on the efficacy of
456 patients receiving immune checkpoint inhibitors in advanced non-small cell lung cancer.

- 457 Cancer Med 2019;8:4023–31. <https://doi.org/10.1002/cam4.2280>.
- 458 [14] Wu Y, Ju Q, Jia K, Yu J, Shi H, Wu H, et al. Correlation between sex and efficacy of
459 immune checkpoint inhibitors (PD-1 and CTLA-4 inhibitors). *Int J Cancer* 2018;143:45–
460 51. <https://doi.org/10.1002/ijc.31301>.
- 461 [15] Zychlinsky Scharff A, Rousseau M, Lacerda Mariano L, Canton T, Consiglio CR, Albert
462 ML, et al. Sex differences in IL-17 contribute to chronicity in male versus female urinary
463 tract infection. *JCI Insight* 2019;5. <https://doi.org/10.1172/jci.insight.122998>.
- 464 [16] Hedegaard J, Lamy P, Nordentoft I, Algaba F, Høyer S, Ulhøi BP, et al. Comprehensive
465 Transcriptional Analysis of Early-Stage Urothelial Carcinoma. *Cancer Cell* 2016;30:27–
466 42. <https://doi.org/10.1016/J.CCELL.2016.05.004>.
- 467 [17] Vidotto T, Nersesian S, Graham C, Siemens DR, Koti M. DNA damage repair gene
468 mutations and their association with tumor immune regulatory gene expression in muscle
469 invasive bladder cancer subtypes. *J Immunother Cancer* 2019;7:148.
470 <https://doi.org/10.1186/s40425-019-0619-8>.
- 471 [18] Wu S-Q, Xu R, Li X-F, Zhao X-K, Qian B-Z. Prognostic roles of tumor associated
472 macrophages in bladder cancer: a system review and meta-analysis. *Oncotarget*
473 2018;9:25294–303. <https://doi.org/10.18632/oncotarget.25334>.
- 474 [19] Martínez VG, Rubio C, Martínez-Fernández M, Segovia C, López-Calderón F, Garín MI,
475 et al. BMP4 Induces M2 Macrophage Polarization and Favors Tumor Progression in
476 Bladder Cancer. *Clin Cancer Res an Off J Am Assoc Cancer Res* 2017;23:7388–99.
477 <https://doi.org/10.1158/1078-0432.CCR-17-1004>.

- 478 [20] Suriano F, Santini D, Perrone G, Amato M, Vincenzi B, Tonini G, et al. Tumor associated
479 macrophages polarization dictates the efficacy of BCG instillation in non-muscle invasive
480 urothelial bladder cancer. *J Exp Clin Cancer Res* 2013;32:87.
481 <https://doi.org/10.1186/1756-9966-32-87>.
- 482 [21] Mantovani A. B cells and macrophages in cancer: yin and yang. *Nat Med* 2011;17:285–6.
483 <https://doi.org/10.1038/nm0311-285>.
- 484 [22] Vidyarthi A, Agnihotri T, Khan N, Singh S, Tewari MK, Radotra BD, et al. Predominance
485 of M2 macrophages in gliomas leads to the suppression of local and systemic immunity.
486 *Cancer Immunol Immunother* 2019;68:1995–2004. [https://doi.org/10.1007/s00262-019-](https://doi.org/10.1007/s00262-019-02423-8)
487 [02423-8](https://doi.org/10.1007/s00262-019-02423-8).
- 488 [23] Mantovani A, Sica A, Sozzani S, Allavena P, Vecchi A, Locati M. The chemokine system
489 in diverse forms of macrophage activation and polarization. *Trends Immunol*
490 *2004;25:677–86*. <https://doi.org/10.1016/j.it.2004.09.015>.
- 491 [24] Fehres CM, van Uden NO, Yeremenko NG, Fernandez L, Franco Salinas G, van
492 Duivenvoorde LM, et al. APRIL Induces a Novel Subset of IgA(+) Regulatory B Cells
493 That Suppress Inflammation via Expression of IL-10 and PD-L1. *Front Immunol*
494 *2019;10:1368*. <https://doi.org/10.3389/fimmu.2019.01368>.
- 495 [25] Birk NM, Nissen TN, Kjærgaard J, Hartling HJ, Thøstesen LM, Kofoed P-E, et al. Effects
496 of Bacillus Calmette-Guérin (BCG) vaccination at birth on T and B lymphocyte subsets:
497 Results from a clinical randomized trial. *Sci Rep* 2017;7:12398.
498 <https://doi.org/10.1038/s41598-017-11601-6>.

- 499 [26] Fink AL, Engle K, Ursin RL, Tang W-Y, Klein SL. Biological sex affects vaccine
500 efficacy and protection against influenza in mice. *Proc Natl Acad Sci U S A*
501 2018;115:12477–82. <https://doi.org/10.1073/pnas.1805268115>.
- 502 [27] Márquez EJ, Chung C-H, Marches R, Rossi RJ, Nehar-Belaid D, Eroglu A, et al. Sexual-
503 dimorphism in human immune system aging. *Nat Commun* 2020;11:751.
504 <https://doi.org/10.1038/s41467-020-14396-9>.
- 505 [28] Porta C, Rimoldi M, Raes G, Brys L, Ghezzi P, Di Liberto D, et al. Tolerance and M2
506 (alternative) macrophage polarization are related processes orchestrated by p50 nuclear
507 factor kappaB. *Proc Natl Acad Sci U S A* 2009;106:14978–83.
508 <https://doi.org/10.1073/pnas.0809784106>.
- 509 [29] Lardone RD, Chan AA, Lee AF, Foshag LJ, Faries MB, Sieling PA, et al. *Mycobacterium*
510 *bovis* Bacillus Calmette-Guérin Alters Melanoma Microenvironment Favoring Antitumor
511 T Cell Responses and Improving M2 Macrophage Function. *Front Immunol* 2017;8:965.
512 <https://doi.org/10.3389/fimmu.2017.00965>.
- 513 [30] Wieland A, Patel MR, Cardenas MA, Eberhardt CS, Hudson WH, Obeng RC, et al.
514 Defining HPV-specific B cell responses in patients with head and neck cancer. *Nature*
515 2020. <https://doi.org/10.1038/s41586-020-2931-3>.
- 516 [31] Kroeger DR, Milne K, Nelson BH. Tumor-Infiltrating Plasma Cells Are Associated with
517 Tertiary Lymphoid Structures, Cytolytic T-Cell Responses, and Superior Prognosis in
518 Ovarian Cancer. *Clin Cancer Res an Off J Am Assoc Cancer Res* 2016;22:3005–15.
519 <https://doi.org/10.1158/1078-0432.CCR-15-2762>.

- 520 [32] Carè A, Bellenghi M, Matarrese P, Gabriele L, Salvioli S, Malorni W. Sex disparity in
521 cancer: roles of microRNAs and related functional players. *Cell Death Differ*
522 2018;25:477–85. <https://doi.org/10.1038/s41418-017-0051-x>.
- 523 [33] Shen Z, Rodriguez-Garcia M, Patel M V, Barr FD, Wira CR. Menopausal status
524 influences the expression of programmed death (PD)-1 and its ligand PD-L1 on immune
525 cells from the human female reproductive tract. *Am J Reprod Immunol* 2016;76:118–25.
526 <https://doi.org/10.1111/aji.12532>.
- 527 [34] Kates M, Matoso A, Choi W, Baras AS, Daniels MJ, Lombardo K, et al. Adaptive
528 Immune Resistance to Intravesical BCG in Non-Muscle Invasive Bladder Cancer:
529 Implications for Prospective BCG-Unresponsive Trials. *Clin Cancer Res an Off J Am*
530 *Assoc Cancer Res* 2020;26:882–91. <https://doi.org/10.1158/1078-0432.CCR-19-1920>.
- 531 [35] DeNardo DG, Ruffell B. Macrophages as regulators of tumour immunity and
532 immunotherapy. *Nat Rev Immunol* 2019;19:369–82. [https://doi.org/10.1038/s41577-019-](https://doi.org/10.1038/s41577-019-0127-6)
533 [0127-6](https://doi.org/10.1038/s41577-019-0127-6).
- 534 [36] Humphrey PA, Moch H, Cubilla AL, Ulbright TM, Reuter VE. The 2016 WHO
535 Classification of Tumours of the Urinary System and Male Genital Organs-Part B:
536 Prostate and Bladder Tumours. *Eur Urol* 2016;70:106–19.
537 <https://doi.org/10.1016/j.eururo.2016.02.028>.
- 538 [37] Pocock SJ, Clayton TC, Altman DG. Survival plots of time-to-event outcomes in clinical
539 trials: good practice and pitfalls. *Lancet (London, England)* 2002;359:1686–9.
540 [https://doi.org/10.1016/S0140-6736\(02\)08594-X](https://doi.org/10.1016/S0140-6736(02)08594-X).

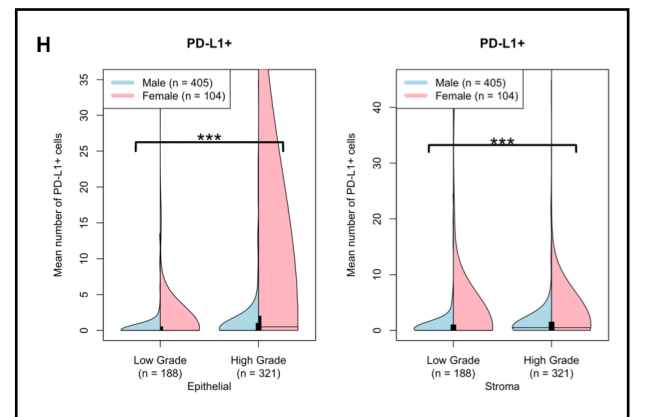
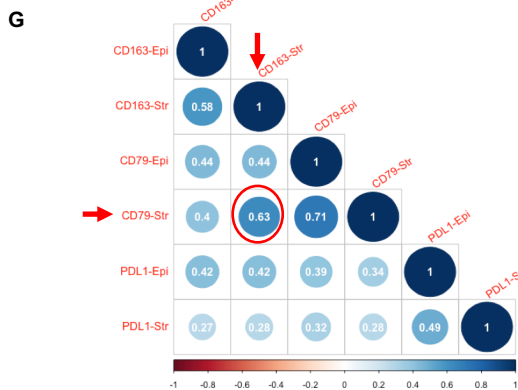
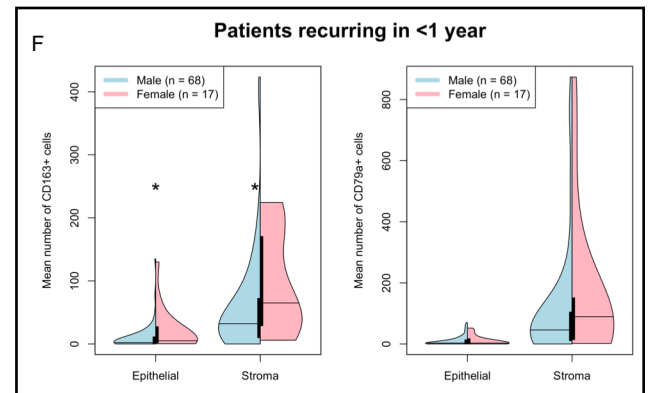
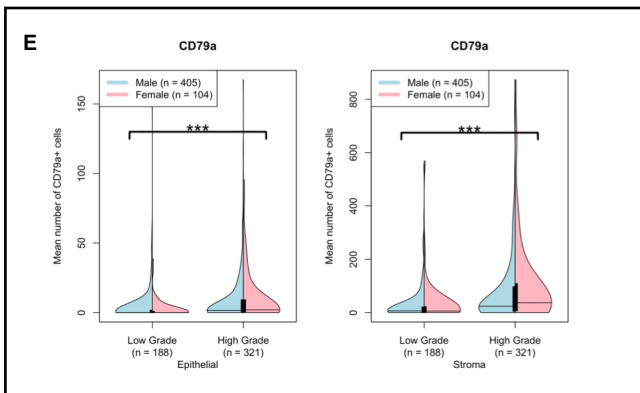
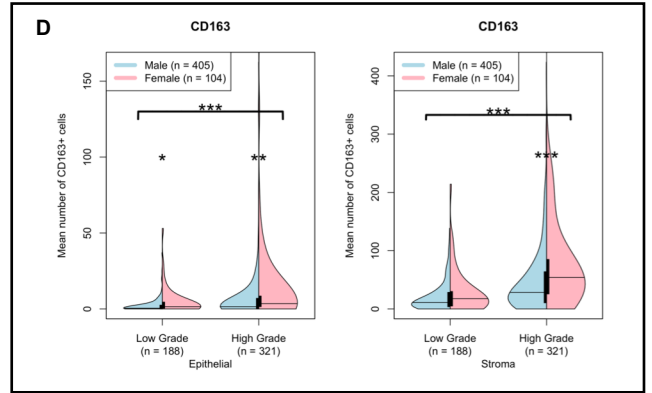
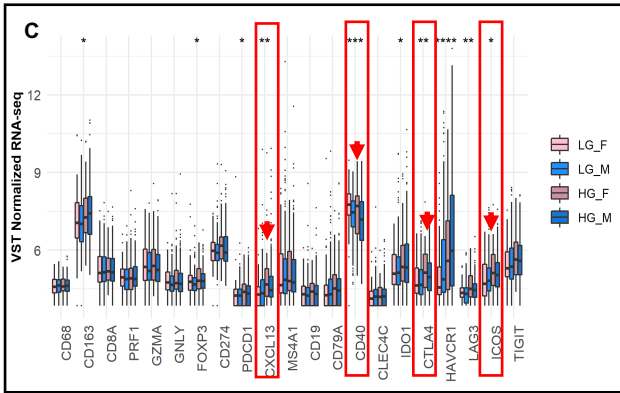
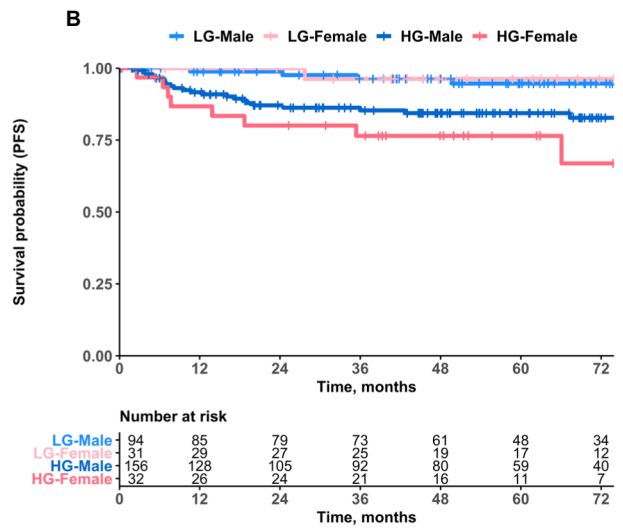
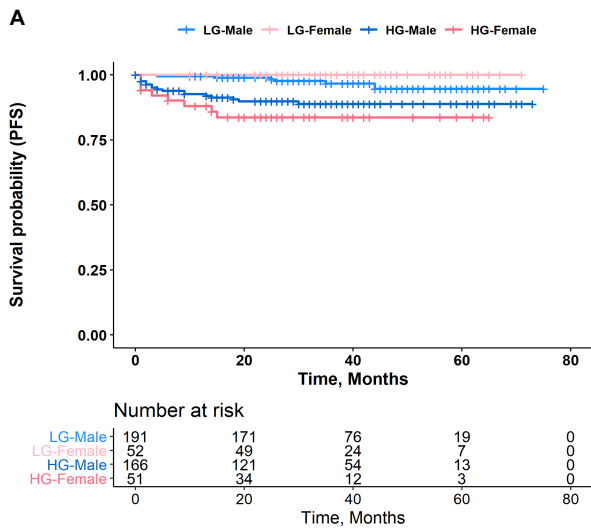


Figure 1. Patients with NMIBC exhibit sexual dimorphism in progression free survival and tumor immune microenvironment.

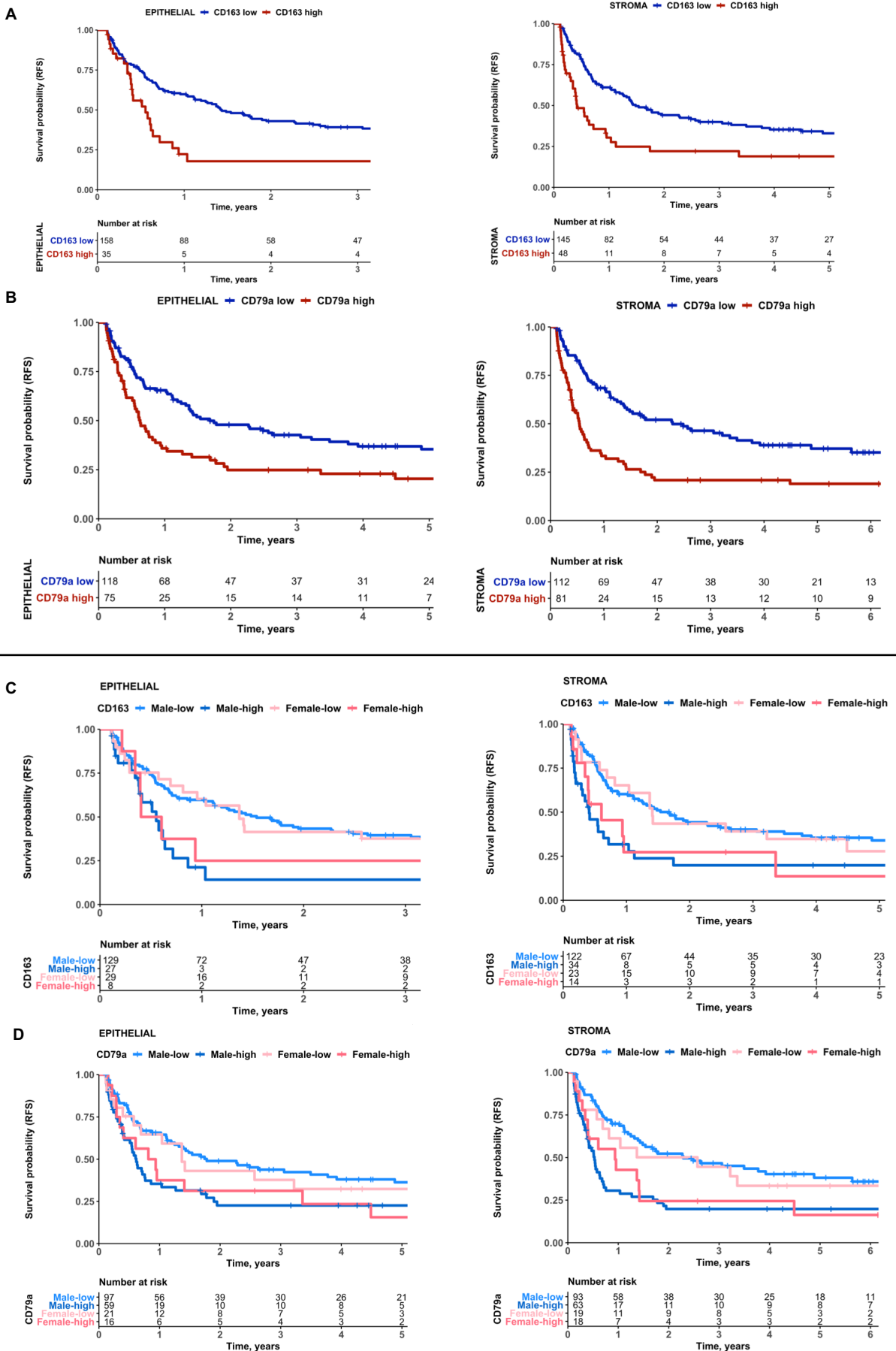


Figure 2. Recurrence free survival (RFS) in high-grade non-muscle invasive bladder cancer is associated with patient sex and tumour immune microenvironment.